BMC Microbiology

RESEARCH Open Access

Screening of biomarkers in acute radiation enteritis based on microbiome and clustering methods

Chenying Ma[1], Xiaoting Xu[1], Songbing Qin[1] and Juying Zhou[1,2*]

Abstract

Background Radiation enteritis (RE) is a common complication of radiotherapy for abdominal and pelvic tumors, adversely affecting treatment outcomes and patients' quality of life. Gut microbiome alterations may contribute to RE development, but the underlying pathogenic factors are not fully understood. This study aimed to characterize the intestinal microbial changes associated with RE and severe acute radiation enteritis (SARE) and to identify predictive biomarkers.

Methods We enrolled 50 cervical cancer patients undergoing radiotherapy and 15 healthy women (controls). Stool samples were collected at the baseline and during weeks 2, 4, and 6 of radiotherapy, and then analyzed using 16 S rDNA sequencing and bioinformatics.

Results Although the Bacteroidetes/Firmicutes (B/F) ratio was higher in patients with RE or SARE, it alone could not predict these conditions. Three enterotypes were identified based on dominant genera: *Blautia* (enterotype 1), *Escherichia-Shigella* (enterotype 2), and *Faecalibacterium* (enterotype 3). A decrease in *Blautia* and an increase in *Escherichia-Shigella* and *Faecalibacterium* were correlated with RE and SARE. Univariate logistic regression revealed that the *Faecalibacterium* enterotype at the baseline was associated with a 4.4-fold higher risk of developing SARE (odds ratio 5.400; $P=0.017$). The *Escherichia-Shigella* enterotype was also linked to increased SARE incidence.

Conclusion These findings suggest that while single bacterial genera or the B/F ratio are insufficient predictors, enterotype classification may serve as a potential biomarker for predicting SARE in patients undergoing radiotherapy.

Keywords Radiation enteritis, Cervical cancer, Intestinal barrier, Microbiome, Clustering methods, Biomarker

*Correspondence:
Juying Zhou
zhoujuyingsy@163.com
[1]Department of Radiation Oncology, the First Affiliated Hospital of Soochow University, Suzhou 215006, China
[2]State Key Laboratory of Radiation Medicine and Protection, Soochow University, Suzhou 215123, China

Introduction

Radiation enteritis (RE) is a frequent and significant complication resulting from radiotherapy in patients with abdominal and pelvic malignancies, notably cervical cancer. It adversely affects treatment efficacy and significantly diminishes patients' quality of life due to symptoms such as abdominal pain, diarrhea, and malabsorption syndromes [1–3]. Despite advancements in radiotherapy techniques, the incidence of RE remains substantial, highlighting the need for a deeper understanding of its pathogenesis and the development of effective preventative and therapeutic strategies [4, 5].

The pathogenic mechanisms underlying RE are complex and multifactorial, involving direct radiation-induced damage to the intestinal epithelium, vascular injury, inflammatory responses, and fibrosis [6, 7]. Recent studies have emphasized the crucial role of the gut microbiome in modulating the host's response to radiation. Radiation can disrupt the intestinal microbial balance, leading to dysbiosis characterized by a reduction in beneficial bacteria and an overgrowth of opportunistic pathogens [8–10]. This dysbiosis can exacerbate mucosal damage, promote inflammation, and impair mucosal healing, thereby contributing to the onset and progression of RE [11, 12].

Current clinical interventions for RE are predominantly symptomatic, focusing on anti-inflammatory medications, mucosal repair agents, electrolyte balance maintenance, and probiotic supplementation [13, 14]. However, these treatments are often insufficient, and early detection and intervention are critical to prevent the progression from acute to chronic RE. The conventional clinical assessment of RE is based on the Radiation Therapy Oncology Group (RTOG) criteria, which may not be sensitive enough for early diagnosis and can yield false-negative results [15]. Therefore, identifying sensitive and specific biomarkers for early detection of RE is of paramount importance.

High-throughput sequencing technologies, particularly 16 S rDNA amplicon sequencing, have revolutionized the study of microbial communities by enabling comprehensive profiling of the microbiome [16]. This method allows for the identification and quantification of bacterial taxa, providing insights into the composition and diversity of the gut microbiome. Recent research has utilized 16 S rDNA sequencing to investigate associations between gut microbiota alterations and gastrointestinal diseases, including radiation-induced enteritis and other inflammatory conditions [17–19].

In this study, we employed 16 S rDNA sequencing to analyze the intestinal microbiome of cervical cancer patients undergoing volumetric modulated arc therapy (VMAT). We aimed to characterize the changes in the gut microbiome associated with RE and severe acute radiation enteritis (SARE) and to identify potential microbial biomarkers for predicting the development of RE. By using clustering methods, we sought to identify specific microbial patterns or enterotypes that could serve as predictive markers, ultimately contributing to improved clinical assessment and early intervention strategies for RE.

Methods

Enrollment

Radiotherapy group

We enrolled 50 patients with cervical cancer treated using pelvic radiotherapy in the Department of Radiotherapy, the First Affiliated Hospital of Soochow University, between August 2017 and August 2018. The inclusion criteria were as follows: [1] 18–80 years of age [2], cervical cancer diagnosed using pathological examination [3], no history of intestinal or metabolic diseases, and [4] good understanding and communication skills. The following exclusion criteria were applied: [1] severe heart, liver, or kidney insufficiency [2], termination of treatment due to serious complications during or after radiotherapy (such as cardiopulmonary, liver, or kidney insufficiency, severe infection, severe bone marrow suppression, massive bleeding, rectovaginal fistula, or vesicovaginal fistula), and [3] refusal to participate in this study.

Control group

We also enrolled 15 healthy women living in Suzhou who served as a control group. The following conditions served as the inclusion criteria: [1] 18–80 years of age [2], body mass index (BMI) of 16.5–25.6 kg/m^2 [3], no history of intestinal diseases, metabolic diseases, malignant tumors, or serious medical disorders [4], no treatment with any antibiotics or probiotics within 3 months before sampling, and [5] good understanding and communication skills. The exclusion criteria were as follows: [1] severe heart, liver, or kidney insufficiency [2], severe chronic diseases such as malignant tumors and autoimmune diseases, within 1 year after sampling, and [3] refusal to participate in this study.

This study was approved by our hospital ethics committee (2016 ethics approval no. 100), and all enrolled subjects provided written informed consent.

Clinical Data

We collected detailed demographic and clinical data from the patients in the radiotherapy group, including name, age, diagnosis, clinical characteristics, sample-collection date, laboratory test results, treatment plan, and contact information. Additionally, we collected general information from the 15 healthy women living in Suzhou (non-minority/ethnicity) who served as a control group,

including name, age, height, weight, personal history, family history, and contact information.

Treatment

Delineation of radiotherapy target area

Magnetic resonance imaging, computed tomography (CT), or positron-emission tomography/CT examinations were routinely performed before treatment for the pre-radiotherapy evaluation. According to the standards of the RTOG [20] and the Japan Clinical Oncology Group [21], the target area and organs at risk (OAR) were delineated for radical radiotherapy and postoperative adjuvant pelvic external irradiation of cervical cancer.

Radiotherapy doses

We prescribed the following doses for radical VMAT: pelvic lymphatic drainage area (planning target volume 1, PTV1), 45 Gy/25 fractions; parametrial area (PTV2), 50 Gy/25 fractions; and positive lymph nodes (PGTVnd), 56 Gy/28 fractions. If tumor progression involved the para-aortic or inguinal lymphatic drainage area, the para-aortic lymphatic drainage area (PTV3) was treated with 36–40 Gy/20 fractions, and the inguinal lymphatic drainage area (PTV4) was treated with 45 Gy/25 fractions.

The doses for postoperative auxiliary VMAT were as follows: medium-risk PTV1, 45 Gy/25 fractions; and high-risk PTV1, 50.4 Gy/28 fractions. The dose for the rest of the target area was prescribed according to the radical external beam irradiation plan.

Designing the radiotherapy plan

The Monaco treatment planning system (Elekta, Sweden) was used to design a 7-field inverse dynamic VMAT plan, according to unified parameters. The X-ray beam voltage was 6 MV. It was required that at least 95% of the PTV receive the prescribed dose, and no dose hot spot ≥ 110% occur outside the PTV. The organ at risk (OAR) dose limit was uniform (OAR dose limitation: bladder V40 < 0%, rectum V40 < 40%, colon V40 < 30%, small intestine V40 < 20%, and femoral head V45 < 5%).

Implementing the radiotherapy plan

VMAT was implemented using the Elekta Synergy linear accelerator (Elekta, Sweden). All patients were treated 5 times a week, once a day with cone-beam CT (Elekta, Sweden) image-guided VMAT. The treatment error was within 3 mm.

Dietary restrictions

Dietary structure was standardized during the radiation treatment. The type and content of dietary ingredients greatly affect the metabolism of the intestinal microbiome. Different dietary structures may also affect the activity of bacterial enzymes in the intestinal microbiome. Bacteria compete with each other for food utilization, and small changes in the diet can significantly alter the metabolism of the gut microbiota. Therefore, in combination with relevant materials such as the Dietary Guidelines for Chinese Residents [22], the Expert Consensus on Nutrition Therapy for Cancer Patients [23], and Nutritional Support for Patients with Radiotherapy [24], standard dietary guidance was drafted under the advice of clinical nutrition specialists to minimize the number of different diets and dietary structures, and thereby minimize the effects of dietary variation on metabolites in biological samples. Both the patients in the radiotherapy group and the control subjects were recommended to follow the standard dietary guidance.

Biological Sample Collection and pretreatment

Stool sample collection

The study participants were instructed to follow the standard dietary plan drawn up by the clinical nutritionist of the hospital. Stool samples were collected after the dietary plan had been followed for 3 consecutive days. In the radiotherapy group, stool samples were collected at the following time points: 1 day before radiotherapy (T0), in the 2nd week (T2) and 4th week (T4) after the start of radiotherapy, and at the end of radiotherapy (Tf). Alterations in the fecal microbiota were assessed using 16 S ribosomal RNA gene (16 S rDNA) amplicon sequencing of stool samples. We compared the intestinal microbial alterations in cervical cancer patients during radiotherapy (T2, T4, and Tf) with the intestinal microbiota before treatment (T0) as well as with the intestinal microbiota in the stool samples collected from the healthy controls.

The sample-collection method was as follows: after all the urine had been expelled, the participant discharged their feces into a spittoon covered with a disposable medical/biological sample-collection bag. The participant then collected approximately 5 g of fresh feces with a disposable sampling spoon, and packed it into two to three 2-mL sterile cryopreservation tubes in order to have backup samples. All the packed cryopreservation tubes were immediately placed in a sampling box and frozen at -80 °C.

Pretreatment and subpackaging

Approximately 2-g portions of the stool specimens were placed in sterile test tubes and stored at -80 °C until analysis. Samples that were contaminated or that had not been collected according to the above requirements were discarded.

Microbiomics Processing Flow

DNA extraction

For DNA extraction, 200 mg of thawed feces was transferred to a 2-mL centrifuge tube and placed on ice. The

FastDNA Spin Kit for Soil was used to extract DNA from the fecal samples, according to the manufacturer's instructions.

Library construction and sequencing

The construction of the high-throughput MetaVx™ sequencing library and sequencing based on the Illumina MiSeq platform were completed by GENEWIZ. The concentration of the library was detected using a Qubit3.0 fluorometer. The library was quantified to 10 nM, and PE250/FE300 paired-end sequencing was performed according to the instructions provided with the Illumina MiSeq instrument. The sequence information was read using the MiSeq Control software that comes with the MiSeq platform. The forward and reverse reads obtained by paired-end sequencing were first assembled and joined in pairs. Sequences containing N in the splicing results were filtered, and sequences with lengths > 200 bp were retained.

Data post-processing

After quality filtering, chimeric sequences were removed, and the final sequence was used for the classification of operational taxonomic units (OTUs). VSEARCH (*v*1.9.6) was used for sequence clustering, with the sequence similarity set to 97%. The results were compared to the 16 S rRNA reference sequences in the Silva 132 database. The Bayesian algorithm, RDP classifier, was used to analyze the species taxonomy of the representative sequences of the OTUs, and the microbial community composition of each sample was counted at different taxonomic levels.

RE evaluation criteria

Adverse reactions were monitored in all patients at the T0, T2, T4, and Tf time points, including diarrhea, abdominal pain, colitis, anal swelling, hematochezia, decreased white blood cell count, decreased neutrophil count, decreased platelet count, and anemia. Adverse events were graded according to the National Institutes of Health Evaluation Criteria for Common Adverse Events (CTCAE *v*5.0) [25]. In this study, the Severe Acute Radiation Enteritis scoring system (SARE-SS) was established based on the adverse reaction score, which was calculated as follows: SARE-SS = the sum of the CTCAE scores of diarrhea + abdominal pain + colitis + anal bloating + blood in the stool. SARE-SS scores ≥ 3 points indicated the occurrence of SARE. The diagnosis of SARE was made by at least 2 experienced radiation oncologists based on changes in the clinical symptoms and the results of ancillary laboratory tests.

Statistical methods

OTU clustering

We used Qiime (*v*1.9.1) and VSEARCH (*v*1.9.6) to classify and identify the intestinal microbiome. In brief, the process involved the following steps: [1] Unique sequences were extracted from the optimized effective sequences, and the number of repetitions of each sequence was noted [2]. Unique sequences with a repetition count of 1 were removed [3]. OTU clustering of the unique sequences (repetition count > 1) was performed with the sequence similarity set to 97%, and chimeric sequences were further removed during the clustering process to obtain representative sequences of the OTUs [4]. All optimized sequences were compared with the representative OTU sequences, and sequences with > 97% similarity with the representative OTU sequences were considered to belong to the same OTU [5]. An OTU abundance table was generated statistically.

Receiver operating characteristic curve analysis

We used R language to analyze receiver operating characteristic (ROC) curves and screen for a single species of the intestinal microbiome that could predict RE and SARE. In brief, we used different cutoff points for the continuous variables and calculated a series of sensitivities and specificities. Then, we plotted curves with sensitivity as the ordinate, and (1 - specificity) as the abscissa. The larger the area under the curve, the higher the diagnostic accuracy.

Enterotype analysis

Using R language, we conducted a cluster analysis of the identified intestinal microbiome to identify the dominant species in RE and SARE. The specific steps were as follows: [1] To calculate the distance matrix, we selected the relative abundance at the genus level, and calculated the Jensen-Shannon divergence between samples [2]. To select the optimal number of clusters, we calculated the Calinski–Harabasz (CH) index, and selected the K value corresponding to the highest CH value, which was the number of sample categories (i.e., the number of clusters) [3]. For sample clustering, the Partitioning Around Medoids algorithm and R language cluster package were used to classify samples according to a predetermined number. Then, the principal component analysis and other graphics were drawn, and group colors were assigned according to the classification results [4]. To evaluate the quality of sample clustering, we calculated the silhouette value of the samples; the higher the silhouette value, the better the sample fit the clustering result.

Statistical analysis

The Kolmogorov-Smirnov test for normality was applied, and normally distributed variables were expressed as

mean ± standard deviation and analyzed using the independent two-samples *t* test. Non-normally distributed variables were expressed as median (interquartile range) and analyzed using the Mann-Whitney *U* test. Pearson correlation analysis was used for normally distributed data, and Spearman correlation analysis was used for non-normally distributed data. In all the above tests, $P<0.05$ was considered to indicate statistical significance.

Results

Clinical characteristics

Of the 50 patients with cervical cancer included in this study, 14 patients received radical radiotherapy, 35 patients received postoperative adjuvant pelvic external beam radiotherapy, and 1 patient received radical pelvic external beam radiotherapy combined with a vaginal brachytherapy boost because the vaginal resection margin was 2 cm from the tumor border. The average patient age was significantly lower in the postoperative adjuvant radiotherapy group than in the radical radiotherapy group ($P<0.05$), while the BMI was significantly higher in the former group than in the latter ($P<0.05$). No significant differences were found in body weight, pathological tumor type, cumulative incidence of RE and SARE, and para-aortic extended field irradiation ($P>0.05$; Table 1) between the radical radiotherapy group and the postoperative adjuvant radiotherapy group.

Table 1 Comparison of general data of patients undergoing postoperative adjuvant radiotherapy and those undergoing radical radiotherapy

Factor	Postoperative adjuvant radiotherapy (*n* = 36)	Radical radiotherapy (*n* = 14)	t/χ^2 value	*P* value
Age (yrs)	48.25 ± 8.05	61.86 ± 13.17	-4.450	< 0.001
Young and middle-aged (18–60 yrs)	33 (92)	5 (36)	17.301	< 0.001
Elderly (> 60 yrs)	3 (8)	9 (64)		
Weight (kg)	57.31 ± 8.00	53.07 ± 8.74	1.638	0.108
BMI (kg/m^2)	21.86 ± 2.07	20.21 ± 2.79	2.284	0.027
Tumor type				0.186*
Squamous cell carcinoma	35 (97)	12 (86)		
Adenocarcinoma	0 (0)	1 (7)		
Adenosquamous carcinoma	1 (3)	1 (7)		
Concurrent chemoradiotherapy			0.397	0.529
Yes	12 (33)	6 (43)		
No	24 (67)	8 (57)		
Paraaortic extended field radiotherapy				0.186*
Yes	1 (3)	2 (14)		
No	35 (97)	12 (86)		
RE			-	1.000*
Yes	30 (83)	12 (86)		
No	6 (17)	2 (14)		
SARE			2.286	0.131
Yes	13 (36)	2 (14)		
No	23 (64)	12 (86)		

*Fisher exact probability method

BMI, body mass index; RE, radiation enteritis; SARE, severe acute radiation enteritis

RE and SARE

None of the 50 cervical cancer patients had any obvious nausea, vomiting, anorexia, dyspepsia, or other gastrointestinal symptoms after the start of VMAT. The following radiotherapy-related adverse reactions were observed in the radiotherapy group: colitis, diarrhea, anal swelling, hematochezia, and bone marrow suppression. No adverse reactions above grade 3 were encountered. The incidence of the symptoms of RE was as follows: diarrhea, 28%; abdominal pain, 22%; colitis, 8%; anal distension, 20%; and blood in stool, 6% in the 2nd week after the start of radiotherapy. The incidence of the above symptoms was 56%, 36%, 16%, 26%, and 18%, respectively, in the 4th week after the start of radiotherapy. The rates of these symptoms peaked at the end of external irradiation, and were 74%, 42%, 24%, 34%, and 30%, respectively. No significant difference in adverse reactions was observed between the radical radiotherapy group and the postoperative adjuvant radiotherapy group (all $P>0.05$; Table 2).

Overview of radiation time/dose-related changes in the intestinal microbiome with RE and SARE

With the advancement of radiotherapy time/dose, the number of *Firmicutes*, *Bacteroidetes*, *Proteobacteria*, and *Actinomycetes* in the intestinal microbiome of the patients with cervical cancer and RE increased. The ratio of *Bacteroidetes*, *Proteobacteria*, and *Actinomycetes* to *Firmicutes* was lower in patients with RE than in patients without RE, and this ratio changed dynamically during radiotherapy (Fig. 1a-e). With the advancement of radiotherapy time/dose, the number of *Firmicutes*, *Bacteroidetes*, *Proteobacteria*, and *Actinomycetes* in the intestinal microbiome of patients with cervical cancer and SARE decreased. The ratio of *Bacteroidetes*, *Proteobacteria*, and *Actinomycetes* to *Firmicutes* was higher in patients with SARE than in patients without SARE, and this ratio changed dynamically during radiotherapy (Fig. 2a-e).

ROC analysis of individual genera reflecting RE and SARE

During radiotherapy, the abundance of *Barnesiella* was significantly lower in the experimental group than in the control group ($P<0.05$, Fig. 3a-d), and the abundance of *Ruminococcus gnavus* and *Erysipelatoclostridium* was significantly higher in the experimental group than in the control group (all $P<0.05$, Fig. 3a-d). In addition, we found that the abundance of the pathogenic bacteria

Table 2 Comparison of the incidence of acute RE in cervical cancer patients treated with postoperative adjuvant radiotherapy (PAR) and radical radiotherapy (RR)

Adverse reaction	Group	Grade 0	Grade 1	Grade 2	Grade 3	χ^2 value	*P* value
Diarrhea	PAR	10 (28)	19 (53)	5 (14)	2 (5)	2.748	0.432
	RR	3 (21)	10 (72)	0 (0)	1 (7)		
Stomach ache	PAR	21 (58)	12 (33)	3 (9)	0 (0)	1.423	0.491
	RR	8 (57)	6 (43)	0 (0)	0 (0)		
Colitis	PAR	25 (69)	11 (31)	0 (0)	0 (0)	-	0.140*
	RR	13 (93)	1 (7)	0 (0)	0 (0)		
Anal Collapse	PAR	22 (61)	9 (25)	5 (14)	0 (0)	1.374	0.503
	RR	11 (79)	2 (14)	1 (7)	0 (0)		
Blood in stool	PAR	23 (64)	13 (36)	0 (0)	0 (0)		0.179*
	RR	12 (86)	2 (14)	0 (0)	0 (0)		
Marrow Inhibition	PAR	12 (33)	9 (25)	10 (28)	5 (14)	3.691	0.297
	RR	3 (21)	4 (29)	2 (14)	5 (36)		

Note: There were 36 patients in the postoperative adjuvant radiotherapy group and 14 patients in the radical radiotherapy group. Values are expressed as number (percentage)

*Fisher exact probability method

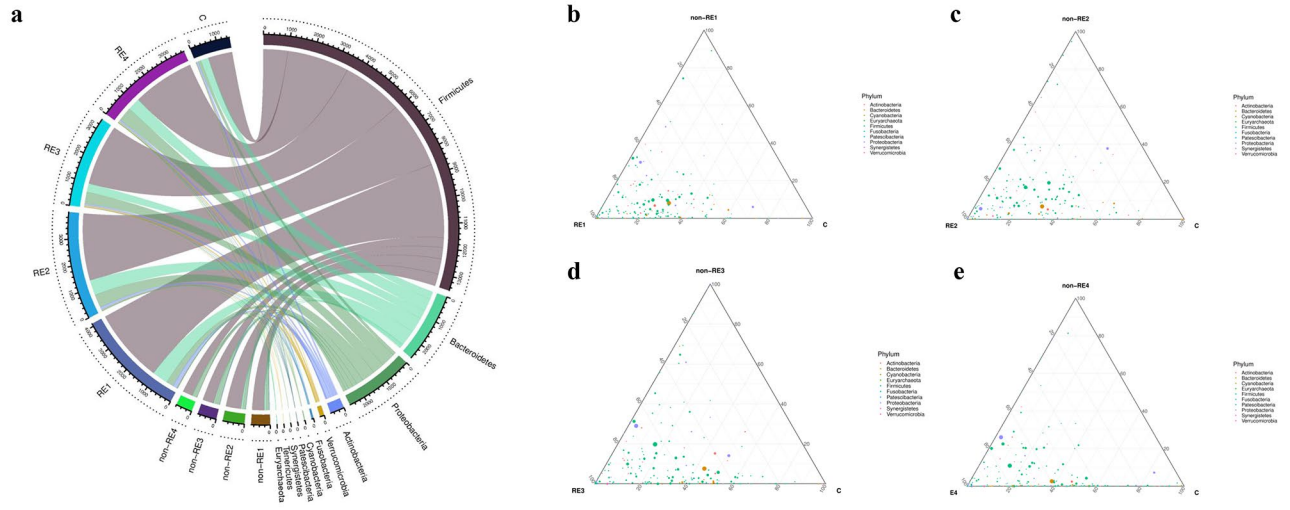

Fig. 1 Overview of radiation time/dose-related changes in the intestinal microbiome in patients with RE. **a**: Chord diagram. **b**–**e**: Ternary phase diagram at time points T0, T2, T4, and Tf. The ratio of Bacteroidetes, Proteobacteria, and Actinomycetes to Firmicutes was lower in patients with RE than in patients without RE, and this ratio changed dynamically during radiotherapy RE, radiation enteritis

Escherichia coli-Shigella and *Tyzzerella-4* in the experimental group increased significantly in the 4th week after the start of radiotherapy (both $P<0.05$, Fig. 3c). The top 10 most abundant species were *Bacteroides*, *Blautia*, *Escherichia-Shigella*, *Faecalibacterium*, *Ruminococcus gnavus*, *Lachnoclostridium*, unclassified bacteria, *Roseburia*, *Eubacterium hallii*, and *Megamonas*. The ROC curve analysis at the genus level for the prediction of RE (Fig. 4a-b) and SARE (Fig. 4c-d) showed that most of the AUC values exceeded 0.5, and all P values exceeded 0.05. So, we considered that a single genus could not predict RE and SARE in our patient group.

Correlation analysis of bacteroidetes/firmicutes ratio reflecting RE and SARE

Some *Bacteroides* species act as probiotics in the host gut. These bacteria produce short-chain fatty acids, such as butyrate [26], which help reduce inflammation and maintain the structural integrity of the gut wall. Therefore, many authors [27–29] believe that a decrease in the ratio of Bacteroidetes to Firmicutes (B/F ratio) may reflect the dysbiosis of the intestinal microbiome and intestinal damage during RE. We found that compared with the control group, the radiotherapy group showed a gradual decrease in the B/F ratio with increase in the radiotherapy dose/time (control: 0.33±0.07 vs. T0: 0.28±0.06 vs. T2: 0.25±0.05 vs. T4: 0.22±0.05 vs. Tf: 0.27±0.07), but no significant difference was found between the groups

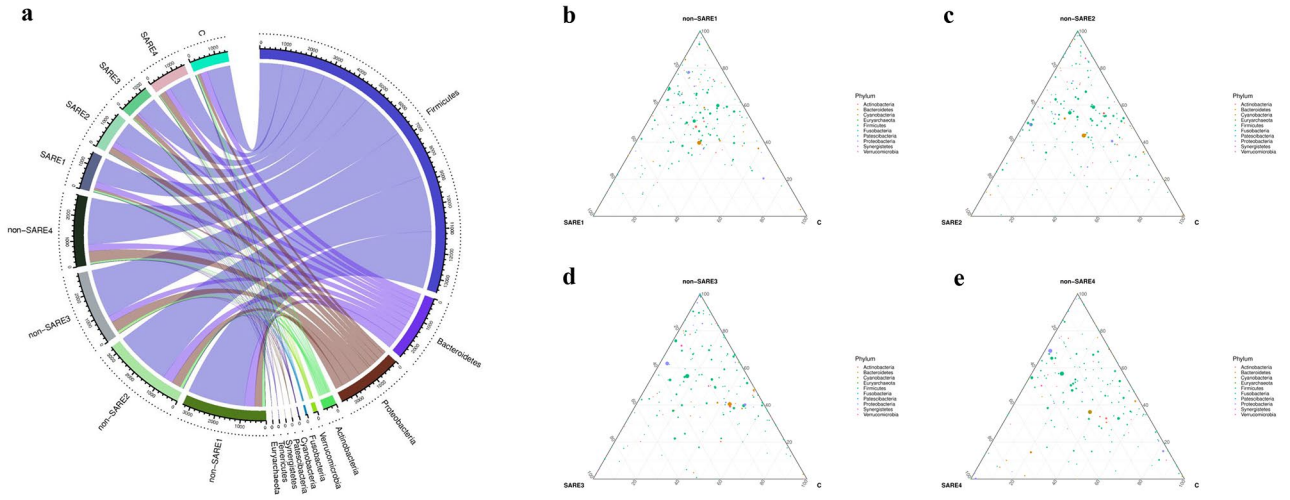

Fig. 2 Overview of radiation time/dose-related changes in the intestinal microbiome in patients with SARE. **a**: Chord diagram. **b**–**e**: Ternary phase diagram at time points T0, T2, T4, and Tf. The ratio of Bacteroidetes, Proteobacteria, and Actinomycetes to Firmicutes was higher in patients with SARE than in patients without SARE, and this ratio changed dynamically during radiotherapy. SARE, severe acute radiation enteritis

($P>0.05$; Fig. 5a). In the radiotherapy group, the B/F ratio was significantly higher among patients with RE and SARE than among patients without RE and SARE, especially in the 2nd week of radiotherapy ($P=0.015$; Fig. 5b) and at the end of radiotherapy ($P=0.002$; Fig. 5c). Using the clustering trend analysis in R software, we divided the patients in the radiotherapy group into 2 clusters (Fig. 5d): cluster 1 consisted of patients with a decreasing B/F ratio, and cluster 2 consisted of patients with an increasing B/F ratio. At the end of radiotherapy, the change in the B/F ratio was significantly greater in cluster 2 than in cluster 1 ($P<0.001$; Fig. 5e). We next studied whether the B/F ratio grouped according to radiotherapy time and the above clusters was correlated with RE and SARE; all the r values were below 0.50, suggesting that the degree of correlation was low, and none of the correlations was statistically significant (all $P>0.05$; Fig. 5f). Therefore, we considered that the B/F ratio alone could not be used as a predictor of RE or SARE.

Enterotype analysis reflecting RE and SARE

The International Human Microbiome Consortium classifies different "gut types" based on differences in the types and quantities of bacteria in the human gut to reflect the dominant microbiome in each ecosystem [30]. For the enterotype analysis in this study, we defined *Blautia* as enterotype 1, *Escherichia-Shigella* as enterotype 2, and *Faecalibacterium* as enterotype 3. Cluster analysis was performed based on the relative abundance data at the genus level (Fig. 6a), and the results were evaluated using the CH index (Fig. 6b). With increase in the radiotherapy time/dose, the enterotypes in the radiotherapy group underwent dynamic changes (Fig. 6c). The proportion of the *Blautia* enterotype shrank, and the proportion of the *Escherichia-Shigella* enterotype gradually increased. In week 4, the incidence of SARE was highest in the *Escherichia-Shigella* enterotype group, and the results were statistically significant (all $P<0.05$; Table 3). *Escherichia-Shigella* is a common intestinal pathogen, and the above results suggest that it is closely related to the occurrence and development of SARE. Univariate logistic regression analysis showed that the *Faecalibacterium* enterotype was associated with an increased incidence of SARE at the baseline (odds ratio = 5.400, $P=0.017$; Table 3), and this enterotype was associated with a 4.4-fold higher risk of SARE than the *Blautia* enterotype.

Discussion

There are as many as 10^{14} bacteria colonizing the adult intestinal tract, with more than 500 distinct species, forming a symbiotic microecological environment composed of anaerobic bacteria, facultative anaerobic bacteria, aerobic bacteria, and the host cells [31]. Endogenous and exogenous influences perturb the microbial abundance and structure Mechanistically, changes in intestinal permeability and dysbiosis of the microbiota can lead to inflammation as well as immune activation and exposure to exogenous effects [32, 33]. In animal experiments, Jahraus et al. [34] found that in fecal samples from normal mice subjected to 550 cGy whole body irradiation, the number of total bacteria, *Bacteroides*, *Streptococcus enterica*, *Lactobacillus*, and Gram-negative anaerobic bacteria were significantly decreased. Sonis et al. [35] confirmed that the intestinal microbiome is partly responsible for the intestinal inflammatory response induced by radiation, which can activate an inflammatory cascade via a signaling pathway mediated by NF-κB.

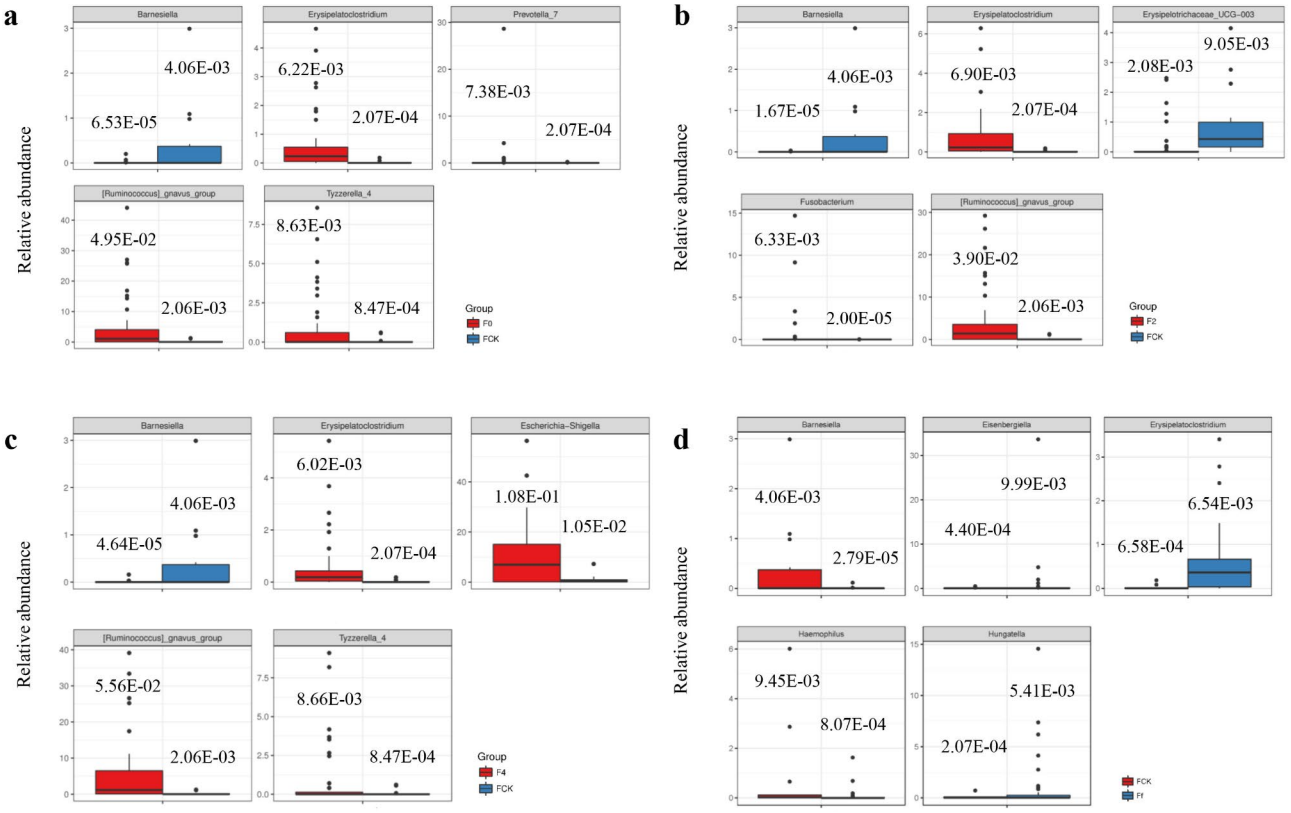

Fig. 3 Dynamic changes in the dominant intestinal microbiome during radiotherapy. **a**: The top 5 bacterial genera with the largest differences in abundance between the radiotherapy group at T0 and the control group were *Barnesiella*, *Erysipelatoclostridium*, *Prevotella_7*, *Ruminococcus gnavus*, and *Tyzzerella-4*. **b**: The top 5 bacterial genera with the largest differences in abundance between the radiotherapy group at T2 and the control group were *Barnesiella*, *Erysipelatoclostridium*, *Erysipelotrichaceae_UCG – 003*, *Fusobacterium*, and *Ruminococcus gnavus*. **c**: The top 5 bacterial genera with the largest differences in abundance between the radiotherapy group at T4 and the control group were *Barnesiella*, *Erysipelatoclostridium*, *Escherichia – Shigella*, *Ruminococcus gnavus*, and *Tyzzerella-4*. **d**: The top 5 species with the largest differences in abundance between the radiotherapy group at Tf and the control group were *Barnesiella*, *Eisenbergiella*, *Haemophilus*, *Hungatella*, and *Erysipelatoclostridium* (all $P < 0.05$). *Note* The figure mainly illustrates the abundance distribution of the 5 most different species between the 2 samples. The taxonomic names of the 5 most different species between the 2 groups of samples are represented by the horizontal axis, and the relative abundance of the species is represented by the vertical axis. Microbiome detection based on 16 S rDNA sequencing was conducted at the following time points in the radiotherapy group: 1 day before radiotherapy (F0), in the 2nd week (F2) and 4th week (F4) after the start of radiotherapy, and at the end of radiotherapy (Ff). Microbiome detection based on 16 S rDNA sequencing was conducted at a single time point in the control group (FCK)

Wright et al. [36] proved that lipopolysaccharide, which is mainly derived from intestinal Gram-negative bacteria, can bind to membrane-associated Toll-like receptors on the surface of innate immune cells to initiate inflammation. In a randomized clinical trial, Manichanh et al. [37] confirmed that radiation could change the abundance and composition of the intestinal microbiome before and after radiotherapy, and this was positively correlated with RE-induced diarrhea. Based on this, it is believed that radiation causes changes in the structure of the intestinal microbiome, leading to the ectopic multiplication of conditional pathogenic bacteria after radiation, which is the root cause of RE and even systemic inflammatory reactions. In this study, we first observed the dynamic changes in the quantity and structure of the gut microbiota in a natural RE model, especially in the populations with RE and SARE, who showed distinct microbiome characteristics.

Studies have confirmed that the gut microbiota can serve as a potential biomarker for RE, and can help guide the creation of a personalized radiation treatment plan. Wang et al. [38] performed 16 S rRNA sequencing of the intestinal microbiota through the Illumina HiSeq platform. The authors observed intestinal microbiome dysbiosis in RE patients, which was characterized by a significant decrease in α-diversity and an increase in β-diversity; specifically, the abundance of the Proteobacteria Gammaproteobacteria was relatively high, and that of Bacteroidetes was low. Patients who later developed RE showed significant enrichment of *Coprococcus* during the baseline period of radiotherapy. Metastat analysis further revealed unique microorganisms associated with the grade of RE, such as an increased abundance

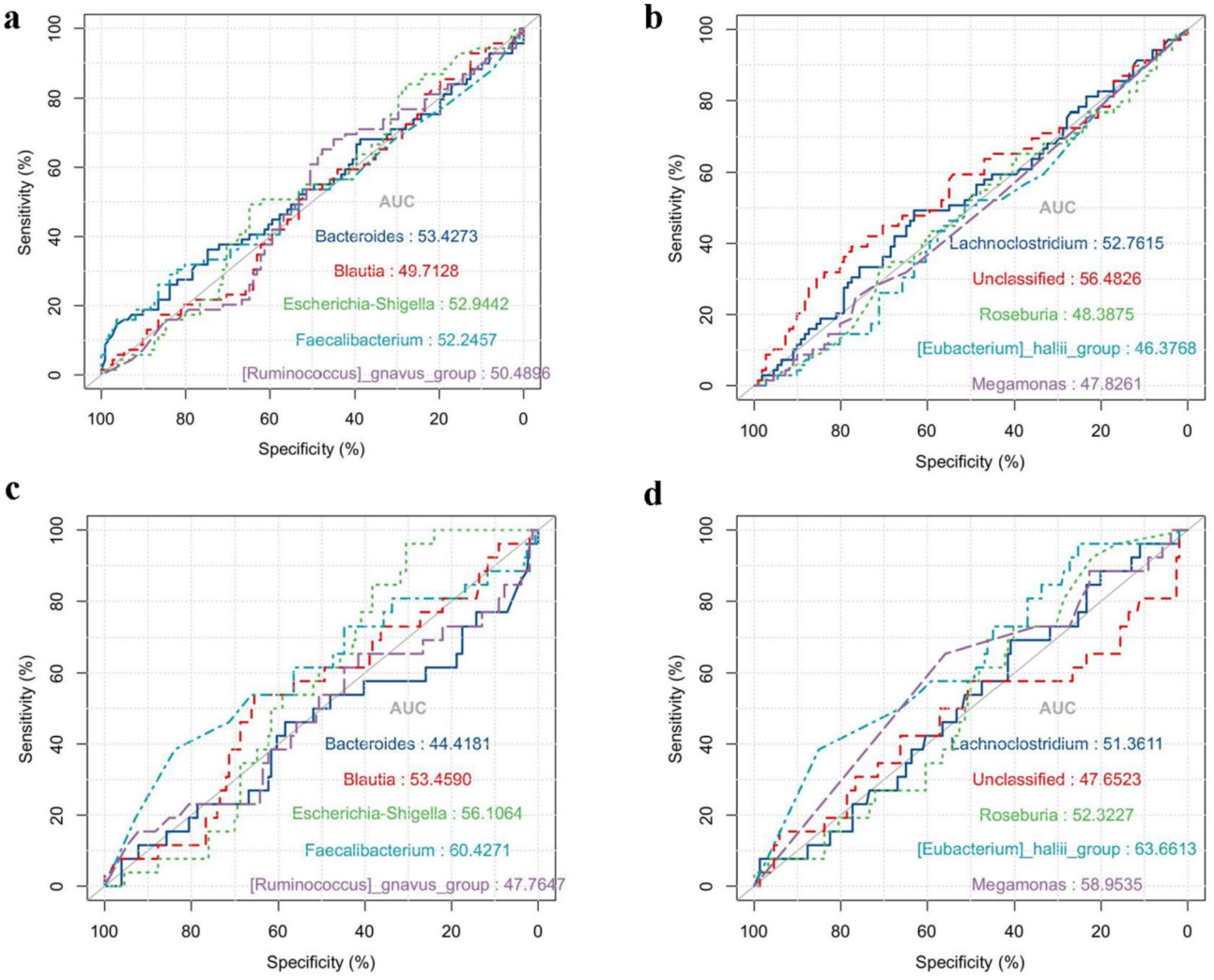

Fig. 4 ROC curve analysis of individual species reflecting RE and SARE. **a**-**b**: RE prediction model. **c**-**d**: SARE prediction model. ROC, receiver operating characteristic; RE, radiation enteritis; SARE, severe acute radiation enteritis

of *Virgibacillus* and *Alcanivorax* in patients with mild enteritis. However, Bosset et al. [39] compared the microbiota at the baseline of radiotherapy, at the end of radiotherapy, and 2 weeks after radiotherapy, and found that actinomycetes increased and *Clostridium* decreased in RE patients. The authors concluded that post-radiation intestinal motility disorders were attributable to Gram-negative bacilli in the gastrointestinal tract. The loss of the intestinal migratory movement complex is a major factor in pathogenic colonization, and it was associated with the increased abundance of Gram-negative bacilli during bacterial overgrowth. In addition, after pathogenic *Escherichia coli* infection, the host cytoskeleton changes, and the absorption surface of the intestinal epithelial cells decreases, resulting in persistent diarrhea. Therefore, the researchers concluded that abnormal intestinal motility and massive colonization by Gram-negative bacilli were important factors for the occurrence of severe late RE [39]. This conclusion is basically consistent with the results of our study. The abundance of gram-negative bacteria such as *Escherichia coli-Shigella* and *Erysipelas* was found to have increased in RE patients; however, this could not be confirmed in the ROC curve analysis, and a single species could not be used as a biomarker to predict RE or SARE.

There are more than 35,000 bacterial species in human intestinal microbiota [40]. Based on dimensional analysis of total bacterial genes, MetaHIT indicates that there are more than 10 million non-redundant genes in the human microbiome. Therefore, it becomes complicated and difficult to grasp the correlations and causal links between diseases and high-dimensional microbiota, and current research favors "dimension reduction" analysis, that is, the identification of representative microbial markers through big data analysis. The gut microbiota is predominantly composed of two major bacterial phyla: Firmicutes

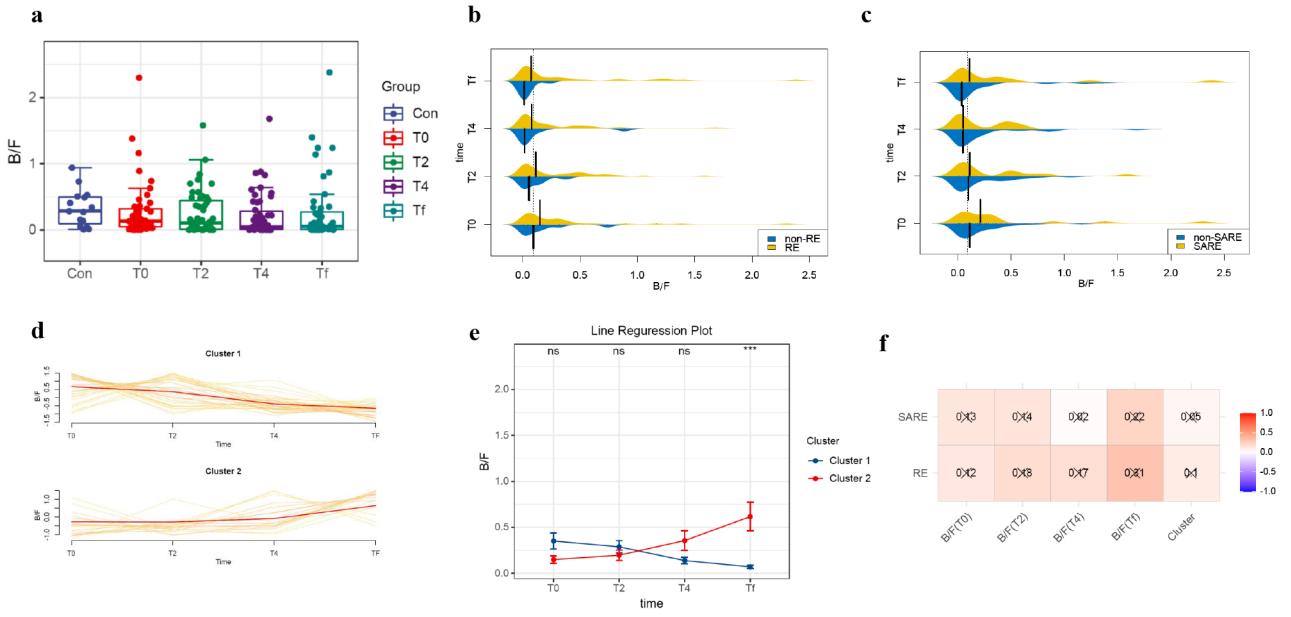

Fig. 5 Analysis of the correlation of the B/F ratio with RE and SARE. **a**: Changes in the B/F ratio between the control group and the radiotherapy group. **b**: Comparison of the B/F ratio between the RE and non-RE populations at different time points. **c**: Comparison of the B/F ratio between the SARE and non-SARE populations at different time points. **d**: Cluster analysis of the B/F ratio of the intestinal microbiome in patients with cervical cancer treated using VMAT. **e**: Comparison of the B/F ratio between 2 types of patients with cervical cancer treated using VMAT at different time points. **f**: Correlation analysis between time classification, cluster classification, and RE and SARE. B/F ratio, Bacteroidetes/Firmicutes ratio; RE, radiation enteritis; SARE, severe acute radiation enteritis; VMAT, volumetric modulated arc therapy

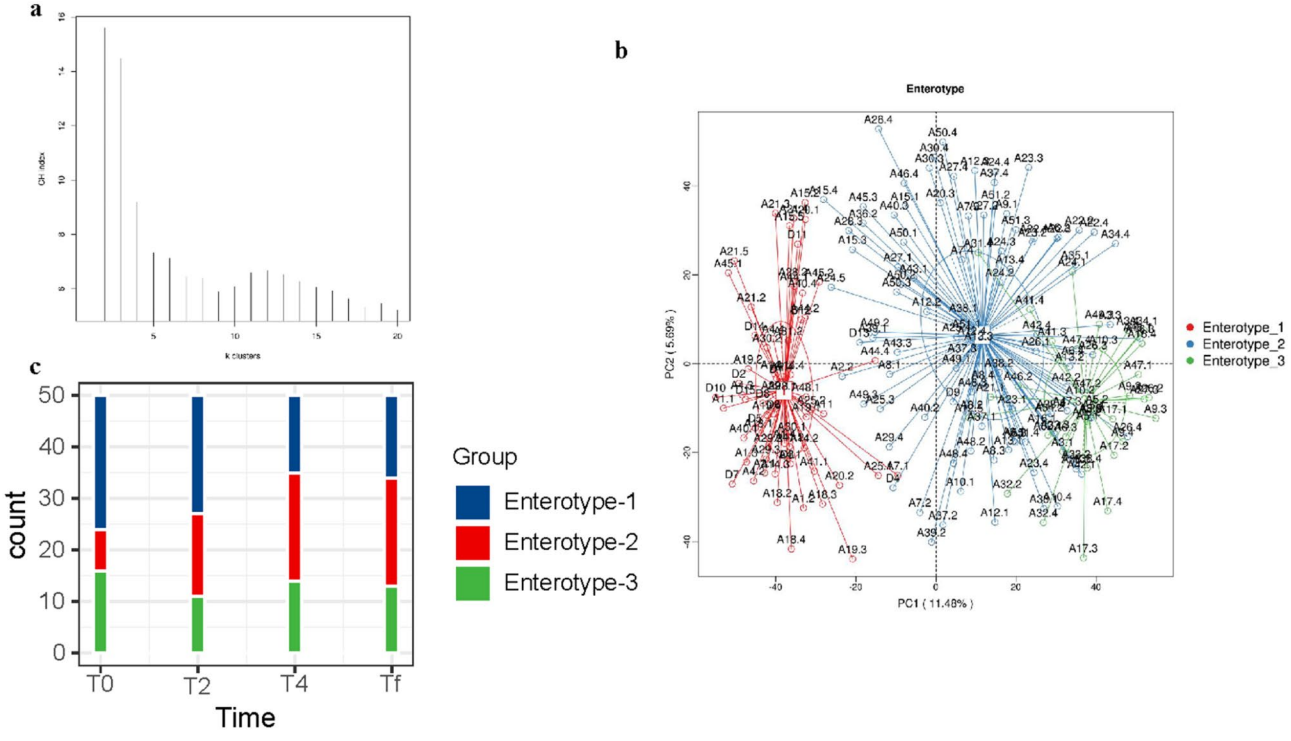

Fig. 6 Enterotype analysis of the included samples. **a**: The horizontal axis represents the number of clusters (K value), and the vertical axis represents the CH index. It is generally believed that the larger the index, the better the clustering effect. The one with the largest CH index among all the genotypes was selected. **b**: Enterotype analysis. Different colors represent different intestinal types. The circle range refers to the PCA diagram that meets the credible interval. c: Diagram showing the distribution of intestinal types at T0, T2, T4, and Tf. CH index, Calinski–Harabasz index; PCA, principal component analysis

Table 3 Univariate analysis of enterotypes in patients with cervical cancer undergoing VMAT

Time	Factor	*B*	*SE*	Exp (B)	95% CI		Wald χ^2	*P*
					Lower	Upper		
T0	Enterotype 1	-	-	1.00	-	-	7.093	0.029
	Enterotype 2	-0.511	1.179	0.600	0.059	6.052	0.188	0.665
	Enterotype 3	1.686	0.708	5.400	1.348	21.639	5.670	0.017
T2	Enterotype 1	-	-	1.00	-	-	5.749	0.056
	Enterotype 2	1.897	0.796	6.667	1.401	31.719	5.683	0.017
	Enterotype 3	1.338	0.881	3.810	0.678	21.419	2.305	0.129
T4	Enterotype 1	-	-	1.00	-	-	0.483	0.785
	Enterotype 2	21.108	103.778	146.861	0.000	175.783	0.000	0.998
	Enterotype 3	20.615	103.778	897.485	0.000	953.054	0.000	0.998
Tf	Enterotype 1	-	-	1.00	-	-	2.488	0.288
	Enterotype 2	0.550	0.802	1.733	0.360	8.351	0.470	0.493
	Enterotype 3	1.312	0.848	3.714	0.704	19.590	2.392	0.122

VMAT, volumetric modulated arc therapy; CI, confidence interval; T0, baseline; T2, 2nd week of radiotherapy; T4, 4th week of radiotherapy; Tf, end of radiotherapy

and Bacteroidetes. Zhong et al. [41] found that a decrease in the B/F ratio reflected the typical features of intestinal microbiome dysbiosis and intestinal damage during RE. The balance between these two groups is crucial for maintaining intestinal homeostasis. An increased B/F ratio indicates a relative abundance of Bacteroidetes over Firmicutes, which can signify a dysbiotic state of the gut microbiome. Our results verified the above finding. The B/F ratio of cervical cancer patients undergoing VMAT gradually decreased with increase in radiation dose/time, but there was no significant difference between the radiotherapy and control groups. In the radiotherapy group, the B/F ratio was significantly higher among patients with RE and SARE than among patients without RE and SARE, especially in the 2nd week of radiotherapy. This may be related to the following mechanisms: An elevated B/F ratio may reflect an increase in Bacteroidetes species, which are associated with pro-inflammatory activities [42]. This shift can exacerbate mucosal damage caused by radiation, leading to increased intestinal permeability and inflammation. Many Firmicutes species are responsible for producing short-chain fatty acids (SCFAs), such as butyrate, which have anti-inflammatory properties and play a key role in maintaining the integrity of the intestinal epithelium [43]. A decrease in Firmicutes abundance could lead to reduced SCFA production, compromising the gut barrier function. Changes in the B/F ratio can alter the production of microbial metabolites that influence the host immune response [44]. An imbalance may promote a microenvironment conducive to the development of RE and SARE. However, when exploring the predictive value of the B/F ratio, we found that the B/F ratio alone could not be used as a predictor of RE or SARE. This indicates that RE and SARE are likely influenced by multiple factors, and relying solely on the B/F ratio may not provide an accurate risk assessment. Hence, we believe the sample size should be enlarged to continue this research.

Some authors have attempted to identify and analyze "intestinal types." The term "enterotype," which first appeared in the journal Nature in 2011, refers to the stratification of the human gut microbiome. Enterotypes can be used to decompose the highly multidimensional human microbiome variation into several categories, and enterotypes can be used as biomarkers to correlate the gut microbiome with phenotypes, including disease phenotypes. Arumugam et al. [45] analyzed 33 qualified samples from different populations, and found that these samples could be divided into 3 different robust clusters at the genus level. Each cluster was then assigned to an enterotype. Common enterotypes included *Bacteroides* (enterotype 1), *Prevotella* (enterotype 2), and *Ruminococcus* (enterotype 3). However, enterotypes are also influenced by age [46], diet [47], and antibiotics [48], among other factors. Some authors believe that the enterotype is not always stable [49]. An enterotype analysis of RE has not yet been reported. In this study, through the Jensen-Shannon divergence cluster scoring method, we defined *Firmicutes* and *Blautia* as enterotype 1, *Proteobacteria* and *Escherichia-Shigella* as enterotype 2, and *Firmicutes* and *Faecalibacterium* as enterotype 3. We also found that the enterotype of some cervical cancer patients undergoing VMAT was not static, but rather changed with the radiation time/dose. The *Faecalibacterium* enterotype could predict the occurrence of SARE in the host. As radiotherapy affects the intestinal mucosa, the abundance and composition of the intestinal microbiome changes over time. The growth of beneficial bacteria can be inhibited, and the reproduction of pathogenic bacteria can be promoted, altering the enterotype of the host. The pathogenic bacteria *Escherichia-Shigella* were related to an increased incidence of SARE during radiotherapy. However, due to a masking effect, the ability of enterotypes to

predict risk is questionable [49], so more research on a larger scale is needed to verify and improve the concept of RE enterotypes.

Conclusion

In conclusion, this study investigated the abundance and composition of the intestinal microbiome, the composition of the dominant microbiome, and the phylogenetics and diversity of the intestinal microbiome by applying next-generation sequencing to analyze the microbiome in stool samples collected from patients with cervical cancer undergoing radiotherapy. Comparative analysis of data collected at the baseline and at different time points throughout radiotherapy showed that the dynamic changes in intestinal microbial profiles after irradiation largely reflected the intestinal microbiome dysbiosis during the evolution of RE. These findings may help to further elucidate the pathogenesis of RE and especially to classify RE enterotypes. The methodological exploration provides new ideas and potential microbiological therapeutic targets for maintaining homeostasis.

Abbreviations

SARE	Severe acute radiation enteritis
VMAT	Volumetric modulated arc therapy
RE	Radiation enteritis
IMRT	Intensity-modulated radiotherapy
SARE-SS	Severe acute radiation enteritis scoring system
CT	Computed tomography
MRI	Magnetic resonance imaging
PET-CT	Positron emission tomography-CT
FIGO	The International Federation of Gynecology and Obstetrics
OAR	Organ at risk
GTV	Gross tumor volume
PTV	Planning target volume
CTV	Clinical target volume
PGTVnd	Metastatic lymph node PTV
CCRT	Concurrent chemoradiotherapy
SCRT	Sequential chemoradiotherapy
BMI	Body mass index
aCCI	age-adjusted Charlson Comorbidity Index
SCC	Squamous cell carcinoma
GTV-nx	The primary tumor GTV
ROC curve	Receiver operating characteristic curve
AUC	The area under the ROC curve
RTOG	Radiation Therapy Oncology Group
OTUs	Operational taxonomic units
CTCAE	Criteria for Common Adverse Events
B/F ratio	Ratio of Bacteroidetes to Firmicutes

Acknowledgements

None.

Author contributions

For transparency, we encourage authors to submit an author statement file outlining their individual contributions to the paper using the relevant CRediT roles: Conceptualization: Ma Chen-ying; Data curation: Ma Chen-ying; Formal analysis: Ma Chen-ying, Xu Xiao-ting; Funding acquisition: Ma Chen-ying, Zhou Ju-ying; Methodology: Ma Chen-ying; Project administration: Zhou Ju-ying, Qin Song-bing; Resources: Zhou Ju-ying, Qin Song-bing; Supervision: Xu Xiao-ting, Qin Song-bing; Validation: Ma Chen-ying; Visualization: Ma Chen-ying; Roles/Writing - original draft: Ma Chen-ying; Writing - review & editing: Ma Chen-ying. Authorship statements should be formatted with the names of authors first and CRediT role(s) following.

Funding

The National Natural Science Foundation of China (no. 81602792), the Natural Science Foundation of the Jiangsu Higher Education Institutions of China (no. 23KJB310023), Jiangsu Provincial Medical Key Discipline (no. ZDXK202235), the Maternal and Child Health Research Project of Jiangsu Province (no. F202210), the Project of State Key Laboratory of Radiation Medicine and Protection, Soochow University (no. GZK1202101), Suzhou Science and Technology Development Plan Project (grant/award no. KJXW2020008), BOXI Natural Science Cultivation Foundation of China of the First Affiliated Hospital of Soochow University (no. BXQN202107), Clinical Diagnosis and Treatment Technology Innovation Project Youth Characteristic Technology Project of the First Affiliated Hospital of Soochow University (no. 2100201).

Data availability

Data related to this study have been uploaded to China National Center for Bioinformation (https://ngdc.cncb.ac.cn/bioproject/). Title: The functional mechanism of gut microbiota in acute radiation enteritis based on metabonomics (PRJCA015092).

Declarations

Ethics approval and consent to participate

This study was approved by our hospital ethics committee (2016 ethics approval no. 100), and all enrolled subjects provided written informed consent. All procedures performed in studies involving human participants were in accordance with the ethical standards of the institutional and/or national research committee and with the 1964 Helsinki declaration and its later amendments or comparable ethical standards.

Consent for publication

Not applicable.

Informed consent

All enrolled subjects provided written informed consent.

Clinical trial number

Not applicable.

Competing interests

The authors declare no competing interests.

Received: 16 January 2024 / Accepted: 4 November 2024
Published online: 08 November 2024

References

1. Moraitis I, Guiu J, Rubert J. Gut microbiota controlling radiation-induced enteritis and intestinal regeneration. Trends Endocrinol Metab. 2023;34(8):489–501.
2. Jian Y, Zhang D, Liu M, Wang Y, Xu ZX. The impact of Gut Microbiota on Radiation-Induced Enteritis. Front Cell Infect Microbiol. 2021;11:586392.
3. Wu J, Ran X, Wang T, Xiong K, Long S, Hao Y, et al. Enteric α-Defensin contributes to recovery of Radiation-Induced Intestinal Injury by modulating gut microbiota and fecal metabolites. Radiat Res. 2024;201(2):160–73.
4. Zhang D, Zhong D, Ouyang J, He J, Qi Y, Chen W, et al. Microalgae-based oral microcarriers for gut microbiota homeostasis and intestinal protection in cancer radiotherapy. Nat Commun. 2022;13(1):1413.
5. Li Y, Dong J, Xiao H, Zhang S, Wang B, Cui M, et al. Gut commensal derived-valeric acid protects against radiation injuries. Gut Microbes. 2020;11(4):789–806.
6. Yang Q, Qin B, Hou W, Qin H, Yin F. Pathogenesis and therapy of radiation enteritis with gut microbiota. Front Pharmacol. 2023;14:1116558.
7. Kumagai T, Rahman F, Smith AM. The Microbiome and Radiation Induced-Bowel Injury: evidence for potential mechanistic role in Disease Pathogenesis. Nutrients. 2018;10(10):1405.
8. Eraqi WA, El-Sabbagh WA, Aziz RK, Elshahed MS, Youssef NH, Elkenawy NM. Gastroprotective and microbiome-modulating effects of ubiquinol in rats with radiation-induced enteropathy. Anim Microbiome. 2024;6(1):40.

9. Wang L, Wang X, Zhang G, Ma Y, Zhang Q, Li Z, et al. The impact of pelvic radiotherapy on the gut microbiome and its role in radiation-induced diarrhoea: a systematic review. Radiat Oncol. 2021;16(1):187.
10. Sokol H, Adolph TE. The microbiota: an underestimated actor in radiation-induced lesions? Gut. 2018;67(1):1–2.
11. He KY, Lei XY, Wu DH, Zhang L, Li JQ, Li QT, et al. *Akkermansia muciniphila* protects the intestine from irradiation-induced injury by secretion of propionic acid. Gut Microbes. 2023;15(2):2293312.
12. Zhu X, Li Y, Tian X, Jing Y, Wang Z, Yue L, et al. REGγ mitigates Radiation-Induced Enteritis by preserving mucin secretion and sustaining Microbiome Homeostasis. Am J Pathol. 2024;194(6):975–88.
13. Zhao Z, Cheng W, Qu W, Shao G, Liu S. Antibiotic alleviates Radiation-Induced Intestinal Injury by Remodeling Microbiota, reducing inflammation, and inhibiting fibrosis. ACS Omega. 2020;5(6):2967–77.
14. Gandle C, Dhingra S, Agarwal S. Radiation-Induced Enteritis. Clin Gastroenterol Hepatol. 2020;18(3):A39–40.
15. Andreyev HJN, Vlavianos P, Blake P, Dearnaley D, Norman AR, Tait D. Gastrointestinal symptoms after pelvic radiotherapy: role for the gastroenterologist? Int J Radiat Oncol Biol Phys. 2005;62(5):1464–71.
16. Wang C, Zhao M, Xie J, Wang H, Gu Z, Sun F. Colon-targeted release of gel microspheres loaded with Antioxidative Fullerenol for Relieving Radiation-Induced Colon Injury and regulating intestinal Microbiome. Adv Healthc Mater. 2023;12(30):e2301758.
17. Zhang L, Miao Z, Li Y, Xu X, Zhou T, Zhang Y, et al. A potential marker of radiation based on 16S rDNA in the rat model: intestinal microbiome. PLoS ONE. 2023;18(8):e0286026.
18. Hu S, Zhou J, Hao J, Zhong Z, Wu H, Zhang P, et al. Emodin ameliorates doxorubicin-induced cardiotoxicity by inhibiting ferroptosis through the remodeling of gut microbiota composition. Am J Physiol Cell Physiol. 2024;326(1):C161–76.
19. Bayram S, Aygün B, Karadayi M, Alaylar B, Güllüce M, Karabulut A. Determination of toxicity and radioprotective properties of bacterial and fungal eumelanin pigments. Int J Radiat Biol. 2023;99(11):1785–93.
20. Small W Jr, Bosch WR, Harkenrider MM, Strauss JB, Abu-Rustum N, Albuquerque KV, et al. NRG oncology/RTOG consensus guidelines for delineation of clinical target volume for intensity modulated pelvic radiation therapy in postoperative treatment of endometrial and cervical cancer: an update. Int J Radiation Oncology* Biology* Phys. 2021;109(2):413–24.
21. Toita T, Ohno T, Kaneyasu Y, Uno T, Yoshimura R, Kodaira T, et al. A consensus-based guideline defining the clinical target volume for pelvic lymph nodes in external beam radiotherapy for uterine cervical cancer. Jpn J Clin Oncol. 2010;40(5):456–63.
22. Wang S-s, Lay S, Yu H-n. Shen S-r. dietary guidelines for Chinese residents (2016): comments and comparisons. J Zhejiang University-SCIENCE B. 2016;17(9):649–56.
23. Bossi P, De Luca R, Ciani O, D'Angelo E, Caccialanza R. Malnutrition management in oncology: an expert view on controversial issues and future perspectives. Front Oncol. 2022;12:910770.
24. Brandhorst S, Longo VD. Fasting and caloric restriction in cancer prevention and treatment. Recent Results Cancer Res. 2016:207:241-66.
25. Basch E, Becker C, Rogak LJ, Schrag D, Reeve BB, Spears P, et al. Composite grading algorithm for the national cancer institute's patient-reported outcomes version of the common terminology criteria for adverse events (PRO-CTCAE). Clin Trails. 2021;18(1):104–14.
26. Fernando MR, Saxena A, Reyes J-L, McKay DM. Butyrate enhances antibacterial effects while suppressing other features of alternative activation in IL-4-induced macrophages. Am J Physiology-Gastrointestinal Liver Physiol. 2016;310(10):G822–31.
27. Khan R, Sharma A, Ravikumar R, Parekh A, Srinivasan R, George RJ, et al. Association between gut microbial abundance and sight-threatening diabetic retinopathy. Investig Ophthalmol Vis Sci. 2021;62(7):19.
28. Ojima M, Motooka D, Shimizu K, Gotoh K, Shintani A, Yoshiya K, et al. Metagenomic analysis reveals dynamic changes of whole gut microbiota in the acute phase of intensive care unit patients. Dig Dis Sci. 2016;61(6):1628–34.
29. Abbas MM, Soto P, Ramalingam L, El-Manzalawy Y, Bensmail H, Moustaid-Moussa N. Sex differences in Fish Oil and Olanzapine effects on Gut Microbiota in Diet-Induced obese mice. Nutrients. 2022;14(2):349.
30. Cheng M, Ning K. Stereotypes about enterotype: the old and new ideas. Genom Proteom Bioinform. 2019;17(1):4–12.
31. Sommer F, Bäckhed F. The gut microbiota—masters of host development and physiology. Nat Rev Microbiol. 2013;11(4):227–38.
32. Jo H, Hwang D, Kim J-K, Lim Y-H. Oxyresveratrol improves tight junction integrity through the PKC and MAPK signaling pathways in Caco-2 cells. Food Chem Toxicol. 2017;108:203–13.
33. Le Dréan G, Haure-Mirande V, Ferrier L, Bonnet C, Hulin P, De Coppet P, et al. Visceral adipose tissue and leptin increase colonic epithelial tight junction permeability via a RhoA-ROCK-dependent pathway. FASEB J. 2014;28(3):1059–70.
34. Jahraus CD, Schemera B, Rynders P, Ramos M, Powell C, Faircloth J, et al. Rifaximin diminishes neutropenia following potentially lethal whole-body radiation. Experimental Biology Med. 2010;235(7):900–5.
35. Stephen TS. The pathobiology of mucositis. Nat Rev Cancer. 2004;4(4):277–84.
36. Ramos SDW, Tobias RA, Ulevitch PS, Mathison RJ. CD14, a receptor for complexes of lipopolysaccharide (LPS) and LPS binding protein. Science. 1990;249(4975):1431–3.
37. Manichanh C, Varela E, Martinez C, Antolin M, Llopis M, Doré J, et al. The gut microbiota predispose to the pathophysiology of acute postradiotherapy diarrhea. Official J Am Coll Gastroenterology| ACG. 2008;103(7):1754–61.
38. Wang Z, Wang Q, Wang X, Zhu L, Chen J, Zhang B, et al. Gut microbial dysbiosis is associated with development and progression of radiation enteritis during pelvic radiotherapy. J Cell Mol Med. 2019;23(5):3747–56.
39. Bosset J, Calais G, Daban A, Berger C, Radosevic-Jelic L, Maingon P, et al. Preoperative chemoradiotherapy versus preoperative radiotherapy in rectal cancer patients: assessment of acute toxicity and treatment compliance: report of the 22921 randomised trial conducted by the EORTC Radiotherapy Group. Eur J Cancer. 2004;40(2):219–24.
40. Frank DN, St. Amand AL, Feldman RA, Boedeker EC, Harpaz N, Pace NR. Molecular-phylogenetic characterization of microbial community imbalances in human inflammatory bowel diseases. Proceedings of the national academy of sciences. 2007;104(34):13780-5.
41. Zhong L, Ma N, Zheng H, Ma G, Zhao L, Hu Q. Tuber Indicum polysaccharide relieves fatigue by regulating gut microbiota in mice. J Funct Foods. 2019;63:103580.
42. Huang F, Zhao R, Xia M, Shen GX. Impact of cyanidin-3-Glucoside on gut microbiota and relationship with metabolism and inflammation in High Fat-High sucrose Diet-Induced insulin resistant mice. Microorganisms. 2020;8(8):1238.
43. Houtman TA, Eckermann HA, Smidt H, de Weerth C. Gut microbiota and BMI throughout childhood: the role of firmicutes, bacteroidetes, and short-chain fatty acid producers. Sci Rep. 2022;12(1):3140.
44. Yang Y, Quan Y, Liu Y, Yang J, Chen K, You X, et al. Exploring the potential mechanism of Xiaojin Pill therapy for benign prostatic hyperplasia through metabolomics and gut microbiota analysis. Front Microbiol. 2024;15:1431954.
45. Arumugam M, Raes J, Pelletier E, Le Paslier D, Yamada T, Mende D. Enterotypes of the human gut microbiome. Nature [Internet]. Nature Publishing Group, a division of Macmillan Publishers Limited. All &#8230.
46. Nakayama J, Yamamoto A, Palermo-Conde LA, Higashi K, Sonomoto K, Tan J, et al. Impact of westernized diet on gut microbiota in children on Leyte Island. Front Microbiol. 2017;8:197.
47. Zhong H, Penders J, Shi Z, Ren H, Cai K, Fang C, et al. Impact of early events and lifestyle on the gut microbiota and metabolic phenotypes in young school-age children. Microbiome. 2019;7(1):1–14.
48. Raymond F, Ouameur AA, Déraspe M, Iqbal N, Gingras H, Dridi B, et al. The initial state of the human gut microbiome determines its reshaping by antibiotics. ISME J. 2016;10(3):707–20.
49. Knights D, Ward TL, McKinlay CE, Miller H, Gonzalez A, McDonald D, et al. Rethinking Enterotypes Cell host Microbe. 2014;16(4):433–7.

Publisher's note